Thermal diffusivity measurement of insulating materials at high temperature with a four-layer (4L) method

Yves Jannot, Alain Degiovanni, Vincent Schick, Johann Meulemans

Thermal diffusivity measurement of insulating materials at high temperature with a four-layer (4L) method

Yves Jannot[1*], Alain Degiovanni[1,2], Vincent Schick[1] and Johann Meulemans[3]

[1] Université de Lorraine, CNRS, LEMTA, F-54500 Vandœuvre-lès-Nancy, France
[2] Université Internationale de Rabat, Pôle Energie, LERMA, Rocade Rabat-Salé, 11100, Sala Al Jadida, Morocco
[3] Saint-Gobain Research Paris, 39 quai Lucien Lefranc, F-93300 Aubervilliers, France

Abstract

This article presents a temperature-temperature thermal characterization method for the measurement of the thermal diffusivity of insulating materials at high temperature. This novel method, noted 4L, is a transient absolute measurement method based on the estimation of the transfer function at the center of a symmetrical stack composed of two specimen of an insulating material sandwiched between two conductive metallic plates. Two different direct 1D semi-analytical models were developed. The first one considers purely conductive opaque materials and the second one takes into account the coupling between radiative and conductive heat transfer modes for purely scattering semi-transparent materials. The first model was used to estimate the thermal diffusivity of two different opaque insulating materials (calcium silicate boards) up to 800°C with accuracy better than 10%. The second model was used to estimate the thermal diffusivity of a semi-transparent insulating material (ceramic foam) up to 1000°C with an accuracy of approximately 10%. The second model was used to identify significant estimation errors occurring if a purely conductive model is used for semi-transparent materials. The conducto-radiative model was also used to estimate an average value of the mean extinction coefficient of the semi-transparent material.

Nomenclature

a	thermal diffusivity [$m^2\ s^{-1}$]
c	specific heat of the sample [$J\ kg^{-1}\ K^{-1}$]
e	thickness of the samples [m]
F	transfer function (real space)
H	transfer function (Laplace space)
L_ν	directional monochromatic radiative intensity [$W\ m^{-1}$]
$L_{0_\nu}(T)$	black body monochromatic radiative intensity at T [$W\ m^{-1}$]
n	refractive index
$P\left(\overrightarrow{\Delta'} \rightarrow \vec{\Delta}\right)$	scattering phase function
p	Laplace parameter [s^{-1}]
q_c	conduction heat flux [$W\ m^{-2}$]

* Corresponding author. Tel: + 33 372 74 43 08. E-mail address : yves.jannot@univ-lorraine.fr (Y. Jannot)

q_r	radiation heat flux [W m^{-2}]
R	radiation resistance [K m^2 W^{-1}]
s	curvilinear coordinate [m]
T	temperature rise [K]
t	time [s]
U	reduced conductance
x	space parameter [m]

Greek symbols

β_ν	monochromatic extinction coefficient [m^{-1}]
β	mean extinction coefficient [m^{-1}]
$\varepsilon_1, \varepsilon_2$	boundaries emissivity
θ	Laplace transform of the temperature rise T
λ	phonic thermal conductivity [W m^{-1} K^{-1}]
λ_{eq}	equivalent thermal conductivity [W m^{-1} K^{-1}]
λ_r	radiative thermal conductivity [W m^{-1} K^{-1}]
Ω	solid angle [sr]
ρ	density [kg m^{-3}]
σ	Stefan-Boltzmann constant [W m^{-2} K^{-4}]
χ_ν	monochromatic absorption coefficient [m^{-1}]
ω_ν	monochromatic scattering albedo

Subscripts

exp	experimental
mod	mode
0	initial value

Abbreviations

GHP	Guarded Hot Plate
HD	Hot Disk
PHW	Parallel Hot-Wire

1. Introduction

Knowledge of the thermal conductivity of high temperature insulating materials is of great importance for the control of industrial processes. For example, the cooling rate of a liquid metal in a mold (which has a great influence on the mechanical properties of the molding) is highly dependent on the thermal resistance of the surrounding insulation. Some ambient temperature reference measurement methods may have limitations when considered for use at high temperatures [1,2]:

- The guarded hot-plate (GHP) method is not used at more than 800°C to our knowledge [3-6].
- The flash method is not suitable for measuring the diffusivity of insulating materials [7,8].
- The hot wire (HW) and the parallel hot wire (PHW) methods allow the measurement of thermal conductivity at high temperatures but only for isotropic materials [9,10]. It was further shown that the hot wire method was not suitable for low density materials [11].
- The hot disk (HD) method can be used up to 800°C but only for isotropic materials and due to the strain exerted on the sensors, the lifetime of mica insulated sensors is limited [12].
- Barth et al [13] proposed a test facility for the measurement of thermal conductivity up to 1650°C using a steady-state method. Satisfying results were obtained but steady state method cannot separate the part of the radiation and of the conduction if case of a scattering material.
- Simmat et al [14] used the Monotonic Heating Method to estimate the thermal diffusivity up to 1600°C. Nevertheless, the non-linearity was taken into account by approximate corrective constants and the radiation transfer was not taken into account.

The method we propose allows to measure the thermal diffusivity of an insulating material at high temperature even if it is anisotropic. Coupled with the measurement of its specific heat by differential or drop calorimetry, this measurement will allow to estimate its thermal conductivity. We will first describe the principle of the proposed method and then the modelling of the direct heat transfer problem will be developed for the following two cases: (1) the material is opaque or (2) the material is a purely scattering semi-transparent material. Experimental measurements carried out up to 1000°C on different insulating materials will be presented and discussed to validate the proposed method.

2. Principle and model

The schematic diagram of the device is presented in figure 1.
It consists of the following elements:

- A plane heating element with a section $S = 30 \times 30\ cm^2$
- Two metal plates with a thickness close to 1 cm and of the same section S as the heating element; their high thermal conductivity ensures a uniform temperature condition at the plate/sample interfaces.
- Two samples of thickness e and section S of the material to be characterized.

The entire device is placed in a furnace maintained at a temperature T_a.

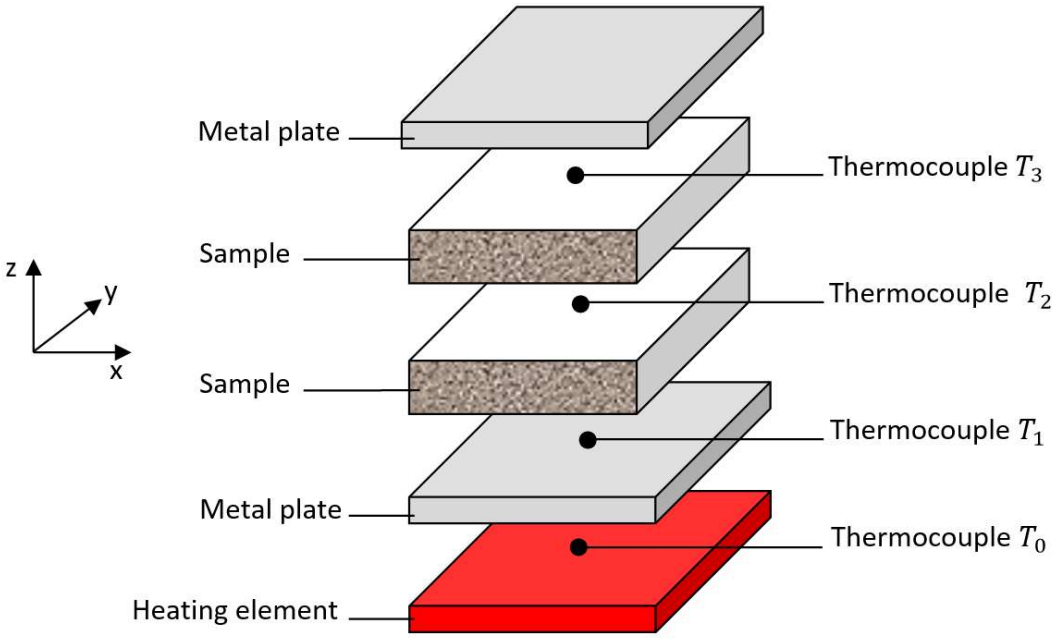

Figure 1: Schematic diagram of the 4L method

The proposed method is a temperature-temperature method [8]: a transfer function between two temperatures instead of a transfer function between a flux and a temperature as done in most conventional methods. This type of method allows minimizing the number of unknown parameters to be estimated [15]. The principle of the method is the following: at the time $t = 0$, when a stationary regime is reached in the system, a modulated heat flow is produced in the heating element and the variations of the three temperatures T_1, T_2 and T_3 are recorded simultaneously. It will be shown that temperature T_2 can be expressed as $T_2(t) = f[T_1(t), T_3(t), a]$ where a is the thermal diffusivity. The thermal diffusivity is considered an unknown parameter. An inverse procedure is carried out to estimate the value which minimizes the quadratic differences between the experimental thermogram and the simulated thermogram calculated with a direct model.

At high temperatures, it is difficult to ensure a uniform temperature throughout the system. At the initial stationary regime, there may be a temperature gradient in the system according to the Oz direction due to external losses (e.g., by the bottom of the furnace on which the heating element is placed). We will therefore make the following assumptions:

- The heat transfer is 1D at the center of the device for the duration of the measurement.
- At the initial time, the temperature profile in the samples is linear.
- The material is opaque.

Initially, it will be assumed that the thermal contact resistances at the various interfaces are negligible. The system to be solved is then written:

$$\frac{\partial^2 T}{\partial x^2} = \frac{1}{a}\frac{\partial T}{\partial t} \quad (1)$$

$$T(0,t) = T_1(t) \quad (2)$$

$$T(2e,t) = T_3(t) \quad (3)$$

$$T(x,0) = T_{01} + \frac{x}{2e}\Delta T \quad (4)$$

with:

$$\Delta T = T_{03} - T_{01} \quad (5)$$

Where:

a thermal diffusivity of the samples ($m^2\ s^{-1}$)

e thickness of the samples (m)

T_{0i} initial value of temperature T_i (K)

We make the following variable change: $\bar{T}(x,t) = T(x,t) - T_{01}$ (6)

The previous relations become:

$$\frac{\partial^2 \bar{T}}{\partial x^2} = \frac{1}{a}\frac{\partial \bar{T}}{\partial t} \quad (7)$$

$$\bar{T}(0,t) = T_1(t) - T_{01} \quad (8)$$

$$\bar{T}(2e,t) = T_3(t) - T_{01} \quad (9)$$

$$\bar{T}(x,0) = \frac{x}{2e}\Delta T \quad (10)$$

Setting: $\theta(x,p) = L[\bar{T}(x,t)]$ (11)

where L is the Laplace transform operator, the heat transfer equation is:

$$\frac{d^2\theta}{dx^2} = \frac{1}{a}[p\theta - \bar{T}(x,0)] = \frac{p}{a}\theta - \frac{x}{2ea}\Delta T \quad (12)$$

The general solution is written as:

$$\theta(x,p) = Acosh(qx) + Bsinh(qx) + \frac{x}{2ep}\Delta T \quad (13)$$

with: $q = \sqrt{\frac{p}{a}}$ (14)

The boundary conditions are:

for $x = 0$: $\theta_1(p) = A$ (15)

for $x = 2e$: $\theta_3(p) = Acosh(2qe) + Bsinh(2qe) + \frac{\Delta T}{p}$ (16)

Hence: $\theta_3(p) = \theta_1(p)cosh(2qe) + Bsinh(2qe) + \frac{\Delta T}{p}$ (17)

and: $B = \frac{\theta_3(p) - \theta_1(p)cosh(2qe) - \frac{\Delta T}{p}}{sinh(2qe)}$ (18)

thus: $\theta(x,p) = \theta_1(p)cosh(qx) + \frac{\theta_3(p) - \theta_1(p)cosh(2qe) - \frac{\Delta T}{p}}{sinh(2qe)}sinh(qx) + \frac{x}{2ep}\Delta T$ (19)

for $x = e$: $\theta(e,p) = \theta_2(p) = \theta_1(p)cosh(qe) + \frac{\theta_3(p) - \theta_1(p)cosh(2qe) - \frac{\Delta T}{p}}{sinh(2qe)}sinh(qe) + \frac{\Delta T}{2p}$ (20)

$$\theta_2(p) = \frac{\theta_1(p) + \theta_3(p)}{2\,cosh(qe)} + \frac{\Delta T}{2p}\left[1 - \frac{1}{cosh(qe)}\right] \quad (21)$$

$$T_2(t) - T_{01} = [T_1(t) + T_3(t) - 2T_{01}] \otimes L^{-1}\left[\frac{1}{2\,cosh(qe)}\right] + \frac{T_{03} - T_{01}}{2} - \frac{T_{03} - T_{01}}{2} \otimes L^{-1}\left[\frac{1}{cosh(qe)}\right] \quad (22)$$

$$T_2(t) - \frac{T_{03} + T_{01}}{2} = [T_1(t) - T_{01} + T_3(t) - T_{03}] \otimes L^{-1}\left[\frac{1}{2\,cosh(qe)}\right] \quad (23)$$

And finally: $T_2(t) - T_{02} = [T_1(t) - T_{01} + T_3(t) - T_{03}] \otimes F(t,a)$ (24)

Where F is the transfer function defined as: $F(t,a) = L^{-1}[H(p)]$ (25)

With: $H(p) = \frac{1}{2\,cosh(qe)}$ (26)

At short times (semi-infinite medium hypothesis for the upper sample), the transfer function has the following simplified form [8]:

$$F(t,a) = L^{-1}[exp(-qe)] = \frac{e}{\sqrt{\pi a t^3}}\ exp\left(-\frac{e^2}{4at}\right) \quad (27)$$

Analysis of the influence of thermal contact resistances

If R_{c1} is the contact resistance between samples and metal plates and $2 \times R_{c2}$ is the contact resistance between the two samples, the following quadrupolar relationships can be written between the lower metal plate and the interface between the two samples on the one hand and between this interface and the upper metal plate on the other hand:

$$\begin{bmatrix}\theta_1\\ \Phi_1\end{bmatrix} = \begin{bmatrix}1 & R_{c1}\\ 0 & 0\end{bmatrix}\begin{bmatrix}A & B\\ C & D\end{bmatrix}\begin{bmatrix}1 & R_{c2}\\ 0 & 1\end{bmatrix}\begin{bmatrix}\theta_2\\ \Phi_2\end{bmatrix} \quad (28)$$

$$\begin{bmatrix}\theta_2\\ \Phi_2\end{bmatrix} = \begin{bmatrix}1 & R_{c2}\\ 0 & 0\end{bmatrix}\begin{bmatrix}A & B\\ C & D\end{bmatrix}\begin{bmatrix}1 & R_{c1}\\ 0 & 1\end{bmatrix}\begin{bmatrix}\theta_3\\ \Phi_3\end{bmatrix} \quad (29)$$

Where: $A = D = cosh(qe)$; $B = \frac{1}{\lambda q} sinh(qe)$; $C = \lambda q sinh(qe)$ and : $q = \sqrt{\frac{p}{a}}$

We obtain a four-equation system. Eliminating Φ_1, Φ_2 and Φ_3 leads to relation (23) as previously but with:

$$H(p) = \frac{1}{2\,[cosh(qe) + qeK\, sinh(qe)]} \quad (30)$$

where $K = \frac{R_{c1}}{\frac{e}{\lambda}}$ is the ratio of the thermal resistances of the contact and of the sample. A remarkable result is that the transfer function does not depend on the contact resistance R_{c2} between the two samples.

The reduced sensitivities of the transfer function to the parameters a and R_{c1} have been calculated for the following extreme cases:

Case 1: $e = 0.03$ m ; $\lambda = 0.1$ W m^{-1} K^{-1} ; $\rho c = 2 \times 10^5$ J m^{-3} K^{-1} (light insulating material)

Case 2: $e = 0.03$ m; $\lambda = 0.8$ W m^{-1} K^{-1}; $\rho c = 7 \times 10^5$ J m^{-3} K^{-1} (refractory)

A very high value of contact resistance: $R_{c1} = 2 \times 10^{-3}$K m^{2}W^{-1}, was considered for both cases. The results are shown in Figure 2.

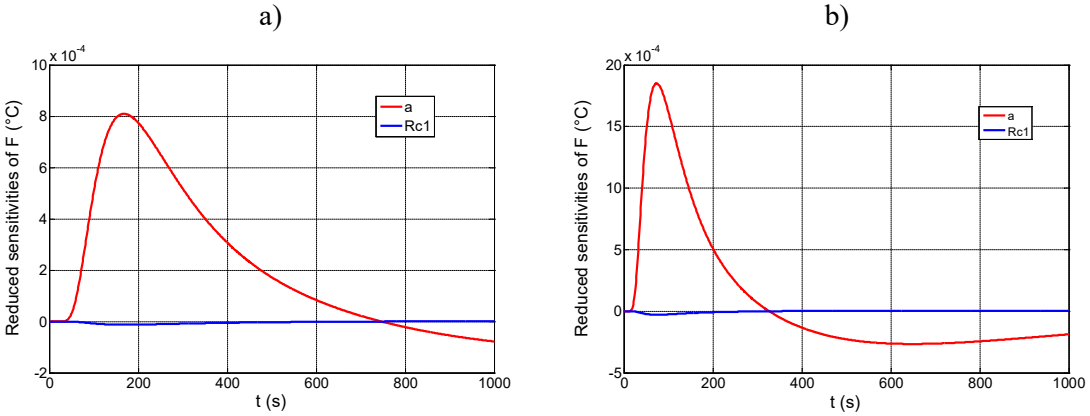

Figure 2: Reduced sensitivities of the transfer function F(t) for: a) Case 1; b) Case 2.

It can be seen that the sensitivity to the contact resistance is low even when considering a very high value of contact resistance. However, to evaluate the influence of this contact resistance on the estimations we carried out simulations of the temperatures T_1, T_2 and T_3 considering a non-zero contact resistance. We then treated these simulated curves as experimental curves to estimate thermal diffusivity using the model which does not take into account contact resistances.

The results obtained are reported in Table 1. It can be noted that the difference between the estimated value and the nominal value is only significant in the case of the highest values where

contact resistance ($R_{c1} = 2 \times 10^{-3}$ K m^{2}W^{-1}) and the thermal conductivity of the sample ($\lambda = 0.8$ W m^{-1} K^{-1}) are high.

Table 1: Estimation deviation for various materials and thermal contact resistances

Values used in the simulation					Estimated value	Deviation
λ	ρc	a	R_{C1}	$K = \frac{R_{c1}}{\frac{e}{\lambda}}$	a	
W m^{-1} K^{-1}	J m^{-3} K^{-1}	m^{2}s^{-1}	K m^{2}W^{-1}		m^{2}s^{-1}	%
0.1	2×10^5	5×10^{-7}	2×10^{-3}	6.67×10^{-3}	4.94×10^{-7}	-1.2
0.1	2×10^5	5×10^{-7}	2×10^{-4}	6.67×10^{-4}	5.00×10^{-7}	0
0.8	7×10^5	1.14×10^{-6}	2×10^{-3}	5.33×10^{-2}	1.03×10^{-6}	-9.6
0.8	7×10^5	1.14×10^{-6}	2×10^{-4}	5.33×10^{-3}	1.13×10^{-6}	-0.9
0.8	7×10^5	1.14×10^{-6}	1×10^{-3}	2.66×10^{-2}	1.08×10^{-6}	-4.8

Figure 3 represents the deviation of the estimation as a function of K.

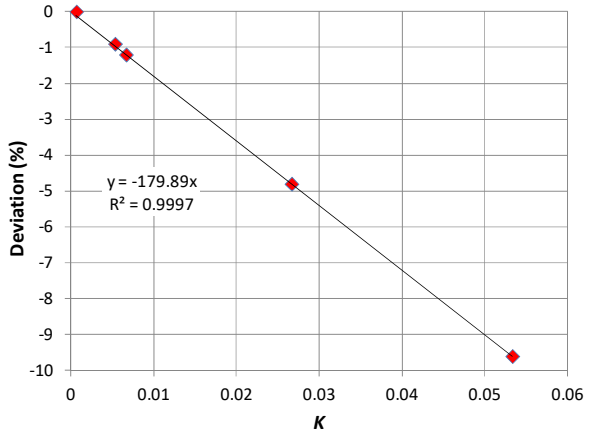

Figure 3 : Deviation of the estimation as a function of the ratio K of the thermal resistances

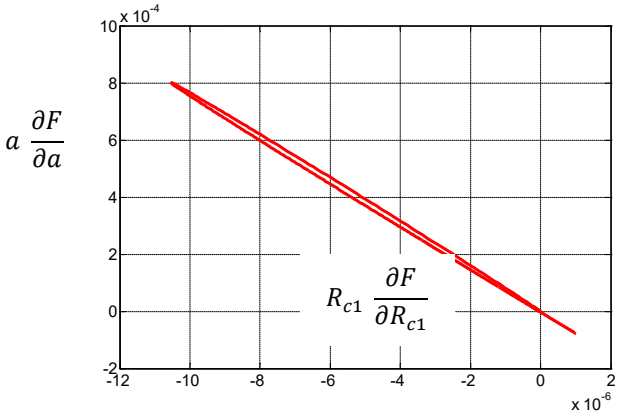

Figure 4: Reduced sensitivity of the transfer function F to a as a function of the reduced sensitivity to R_{C1} (case 1)

It shows that:

- The deviation is perfectly proportional to the value of K (correlation coefficient $R^2 = 0.9997$)
- K must be lower than 5.6×10^{-3} to obtain a deviation lower than 1%.

One can then wonder whether it would be relevant to simultaneously estimate both the thermal diffusivity and the thermal contact resistance. Figure 4 represents the reduced sensitivity of the transfer function F to a as a function of the reduced sensitivity of F to R_{C1} for case 1. It shows that the two sensitivities are perfectly correlated so that it is impossible to estimate them separately.

Case of a purely scattering semi-transparent medium

In general, the energy balance and the radiative balance can be written in the following forms [16]:

$$\rho c \frac{\partial T}{\partial t} = -div(\overrightarrow{q_c} + \overrightarrow{q_r}) \quad (31)$$

where:

$$\overrightarrow{q_c} = -\| \lambda \| \overrightarrow{grad}(T) \text{ (conduction flux density vector)} \quad (32)$$

$$\overrightarrow{q_r} = \int_0^\infty \int_{4\pi} L_\nu(s, \vec{\Delta})\vec{\Delta}\, dr\, d\Omega \text{ (radiation flux density vector)} \quad (33)$$

And:

$$\frac{1}{\beta_\nu}\frac{dL_\nu(s,\vec{\Delta})}{ds} + L_\nu(s, \vec{\Delta}) = (1-\omega_\nu)n^2 L_{0_\nu}(T) + \frac{\omega_\nu}{4\pi}\int_{4\pi} P\left(\overrightarrow{\Delta'} \to \vec{\Delta}\right) L_\nu\left(s, \overrightarrow{\Delta'}\right) d\Omega \quad (34)$$

with:

L_ν	directional monochromatic radiative intensity (W m^{-1})
s	curvilinear coordinate (m)
β_ν	monochromatic extinction coefficient (m^{-1})
ω_ν	monochromatic scattering albedo
n	refractive index
ν	frequency (m^{-1})
$L_{0_\nu}(T)$	black body monochromatic luminance at T (W m^{-1})
$P\left(\overrightarrow{\Delta'} \to \vec{\Delta}\right)$	scattering phase function
Ω	solid angle

And: $$div(\overrightarrow{q_r}) = 4\pi \int_0^\infty \chi_\nu n^2 L_{0_\nu}(T)\, d\nu - \int_0^\infty \chi_\nu \int_{4\pi} L_\nu(s, \vec{\Delta})\, d\Omega\, d\nu \quad (35)$$

With:

χ_ν	monochromatic absorption coefficient (m^{-1})

In the general case the two equations (31) and (34) are coupled because the luminance is involved in the energy balance and the temperature in the radiative balance.

In the case of a purely scattering medium, $\omega_\nu = 1$ and $\chi_\nu = 0$, therefore:

$$div(\overrightarrow{q_r}) = 0 \quad (36)$$

The energy balance becomes:

$$\rho c \frac{\partial T}{\partial t} = -div(\overrightarrow{q_c}) \quad (37)$$

The radiative balance becomes:

$$\frac{1}{\beta_\nu}\frac{dL_\nu(s,\vec{\Delta})}{ds} + L_\nu(s,\vec{\Delta}) = \frac{1}{4\pi}\int_{4\pi} P\left(\overrightarrow{\Delta'} \to \vec{\Delta}\right) L_\nu\left(s,\overrightarrow{\Delta'}\right) d\Omega \quad (38)$$

The last two equations are completely decoupled, the energy balance is the same as for a purely conductive transfer and the radiative balance is independent of the temperature (it depends only on the radiative characteristics of the medium and of the radiative conditions at the limits).

The divergence of the radiative flux being zero, one is in the presence of a flux tube with a conservative flux; the medium therefore behaves as a resistance with respect to the radiative flux. If we also make the hypothesis of opaque limits we can write:

$$T_1 - T_2 = R\, q_r \quad (39)$$

With:

T_1, T_2 temperatures at the boundaries (K)

R radiative resistance (K m^2 W^{-1})

The medium can therefore be formally represented by a quadrupole $\begin{bmatrix} A & B \\ C & D \end{bmatrix}$ in parallel with a resistance R. This association is equivalent to the single quadripole $\begin{bmatrix} A' & B' \\ C' & D' \end{bmatrix}$ whose coefficients can be calculated by the following relationships [17]:

$$A' = D' = \frac{AR+B}{R+B} \quad (40)$$

$$B' = \frac{BR}{R+B} \quad (41)$$

$$C' = \frac{CR+2A-2}{R+B} \quad (42)$$

Given these relationships, the transfer function of the 4L method is then written:

$$F(t,a,U) = L^{-1}\left[\frac{1}{2}\,\frac{1+U\dfrac{sinh\left(\sqrt{\frac{p}{a}}\,e\right)}{\sqrt{\frac{p}{a}}\,e}}{cosh\left(\sqrt{\frac{p}{a}}\,e\right)+U\dfrac{sinh\left(\sqrt{\frac{p}{a}}\,e\right)}{\sqrt{\frac{p}{a}}\,e}}\right] \quad (43)$$

Where U is the reduced conductance defined by: $U = \frac{e}{R\lambda S}$ (44)

where λ is the phonic thermal conductivity. The phonic thermal conductivity corresponds to the 'true' thermal conductivity of a material and is different from the equivalent thermal conductivity of a material if several heat transfer modes play a role (e.g., coupling between conduction and radiation for semi-transparent materials).

If the radiation resistance is put in the form: $R = \frac{e}{\lambda_r S}$ (45)

We obtain: $U = \frac{\lambda_r}{\lambda}$ (46)

Where λ_r represents the part of radiation in the heat transfer that we will refer to as radiative conductivity.

The two estimable parameters are therefore $a = \frac{\lambda}{\rho c}$ and $U = \frac{\lambda_r}{\lambda}$. In this case it can be seen that the equivalent thermal conductivity $\lambda_{eq} = \lambda + \lambda_r$ can be estimated only if the volume heat capacity ρc is known.

3. Parameters estimation

The temperature $T_2(t)$ can be calculated by relation (24) where $F(t)$ is calculated by an inverse

Laplace transform applied to $H(p)$, using the De Hoog algorithm [18]. The estimation procedure uses a Levenberg-Marquardt algorithm [19] to find the values of the unknown parameters which minimize the sum of the quadratic errors:

$$S = \sum_{n=1}^{N} \left[T_{2_{exp}}(t) - T_{2_{mod}}(t) \right]^2 \quad (47)$$

$$\text{Where : } T_{2_{mod}}(t) = T_{02_{exp}} + \left[T_{1_{exp}}(t) - T_{01_{exp}} + T_{3_{exp}}(t) - T_{03_{exp}} \right] \otimes F(t, a) \quad (48)$$

And N is the number of experimental points.

In the case of an opaque medium, it is important to note that the only unknown parameter to be estimated is the thermal diffusivity whereas three parameters must be estimated in the conventional flash method [8].

Analysis of 3D effects

As already done in [20], 3D simulations of the system were carried out with COMSOL to verify that the heat transfer at the center of the stack with a cross section 0.3 × 0.3 m^2 is 1D when the thickness of the samples is lower than 0.03m.

4. Materials and method

First, we will describe the elements of the device schematically represented in Figure 1.
The heating element consists of a 316L steel plate 10 mm-thick and 300 × 300 mm^2 cross-section in which a 2 × 2 mm^2 square-section groove was machined according to the plan of Figure 5. A heating element of 4 m length insulated in an Inconel sheath with an outside diameter of 2 mm is inserted into this groove.

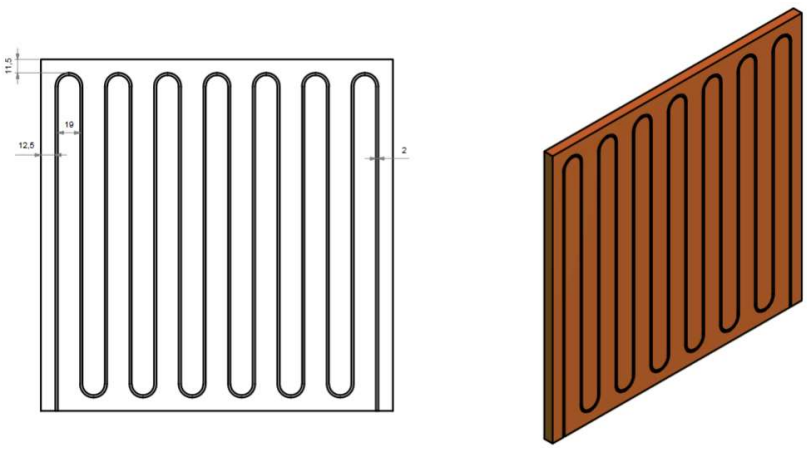

Figure 5: Schematic view of the heating plate

The two metal plates on either side of the samples are made of Nickel, section 300 × 300 mm^2 and thickness 9 mm. A groove of section 0.5 × 0.5 mm^2 is made on the lower side of the bottom plate. A K-type thermocouple with an external diameter of 0.5 mm is inserted into this groove to measure the temperature $T_0(t)$. The thermocouple is connected to a Watlow regulator that controls the heating power. A 0.5 × 0.5 mm^2 cross-section groove is also practiced on the underside of the top plate. A 0.5 mm outer diameter sheathed K-type thermocouple is inserted into this groove and connected to the Picolog-TC08 recording module to measure the temperature $T_3(t)$ with a time step of 0.1s.

A 0.5 × 0.5 mm^2 cross-section groove and 150 mm in length, with the end at the center of the face, was realized on each side of the lower sample. A thermocouple is placed in each of the two grooves to measure the temperatures $T_1(t)$ and $T_2(t)$.
Both sides of the plates are covered with a thin coat of matt black paint resistant up to 1000°C. This experimental device was used in an experimental study to confirm the theoretical results. Measurements were conducted on the following high temperature insulating materials: Silcal 1100 (a calcium silicate board by Silca refractory solutions), LUX500 (a calcium silicate board by Final Advanced Materials) and Norfoam (a ceramic foam by Saint-Gobain).
Our measurements were undertaken between 200 and 800°C for Silcal 1100, between 200 and 500°C for LUX 500 and between 400 and 1000°C for Norfoam.
Silcal 1100 is a calcium silicate based material. It is a light-weight high temperature insulating material, its density, estimated by weighing and measuring the dimensions of the samples, is 245 kg m^{-3}. The thermal conductivity of Silcal 1100 at various temperatures was measured by several laboratories [21]. The results have been confirmed recently by Jannot and Degiovanni [10] who have established the following relation valid between 300 and 1100K:

$$\lambda = 0.06797 + 3.699 \times 10^{-5}\, T + 6.202 \times 10^{-8}\ T^2 - 8.502 \times 10^{-12}\ T^3 \quad (49)$$

Where T is the absolute temperature in K.
Ohmura et al. [22] measured the specific heat c (J kg^{-1} K^{-1}) of the calcium silicate by drop calorimetry and they proposed the following relation valid between 100°C and 1000°C :

$$c = 439 + 82.9 \times ln(T) \quad (50)$$

Where T is the absolute temperature in K
LUX 500 is a high temperature insulating material (calcium silicate board), its density, estimated by weighing and measuring the dimensions of the samples, is 770 kg m^{-3}. Its thermal conductivity was measured by a guarded hot plate (GHP) up to 525°C at LNE [23] and its specific heat was measured by a Setaram calorimeter. The values and the estimated uncertainties are given in table 2.

Table 2: Thermal properties of LUX 500 measured by GHP and calorimetry.

T	ρ	c	λ	a
		Calorimeter (±5%)	GHP (±5%)	$a = \frac{\lambda}{\rho c}$ (±10%)
°C	kg m^{-3}	J kg^{-1} K^{-1}	W m^{-1} K^{-1}	m^{2}s^{-1}
175	770	876	0.210	3.10×10^{-7}
325	770	891	0.213	3.11×10^{-7}
525	770	911	0.199	2.84×10^{-7}

Norfoam® is a fiber free insulation refractory ceramic foam developed by Saint-Gobain. Norfoam® is used for high temperature insulation markets (maximum temperature range between 1200 and 1800°C). It is an open-cell ceramic foam, made of ultra-pure alumina (>99.5 wt% Al_2O_3), with a nominal porosity around 82%. Its density is $\rho = 700$ kg m^{-3} and its equivalent thermal conductivity measured by the parallel hot wire method (ISO standard 8894-2)[9] is $\lambda = 0.75$W m^{-1} K^{-1} at 800°C and $\lambda = 0.80$ W m^{-1} K^{-1} at 1000°C. The specific heat and thermal conductivity of alumina is given by [24], [25]:

$$c = 1.0446 + 1.742 \times 10^{-4}\, T - 2.796 \times 10^{4}\, T^{-2} \quad (51)$$

$$\lambda = 5.5 + 34.5 \times exp(-0.0033\, T) \quad (52)$$

Where T is the temperature (°C).

5. Results and discussion

Results for Silcal 1100

Figure 6 provides an example of an experimental record of temperatures T_1, T_2 and T_3 obtained with Silcal 1100.

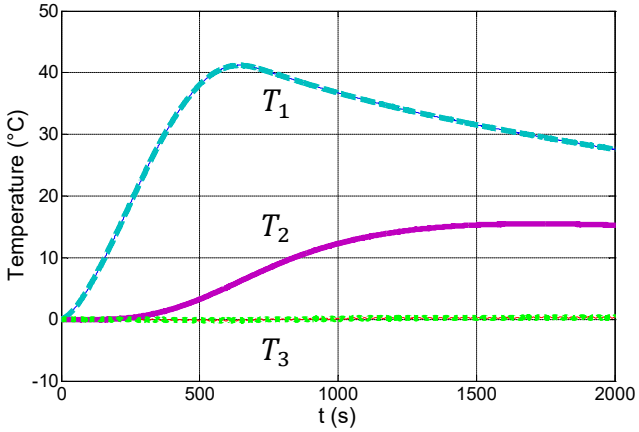

Figure 6: Example of an experimental record of temperatures T_1, T_2 and T_3 obtained with Silcal 1100.

The estimation has was carried out over a time interval [0, 1000 s] after analysis of the value of the transfer function F and of the reduced sensitivity of the temperature T_2 to the thermal diffusivity a, both of which reach their maximum around 700 s as shown in Figure 7 obtained for Silcal 1100.

Figure 8 shows an example of the estimation results from an experimental curve with two very different time intervals. The residues are a little less flat when the time interval increases but remain very satisfactory. It can therefore be concluded that the assumptions of the model are verified, in particular the hypothesis of a 1D transfer to the center of the sample.

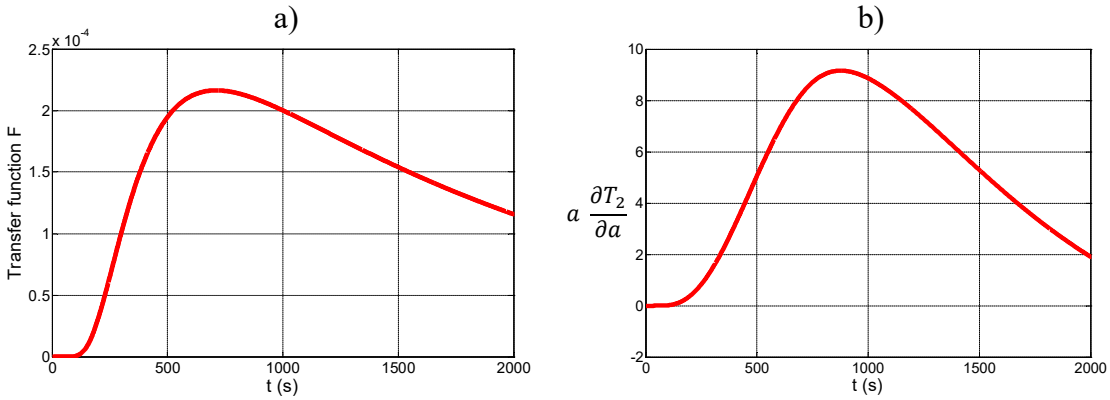

Figure 7: Simulated curves obtained for Silcal 1100 at 800°C: a) Transfer function (t) ; b) Reduced sensitivity of the temperature T_2 to the thermal diffusivity a

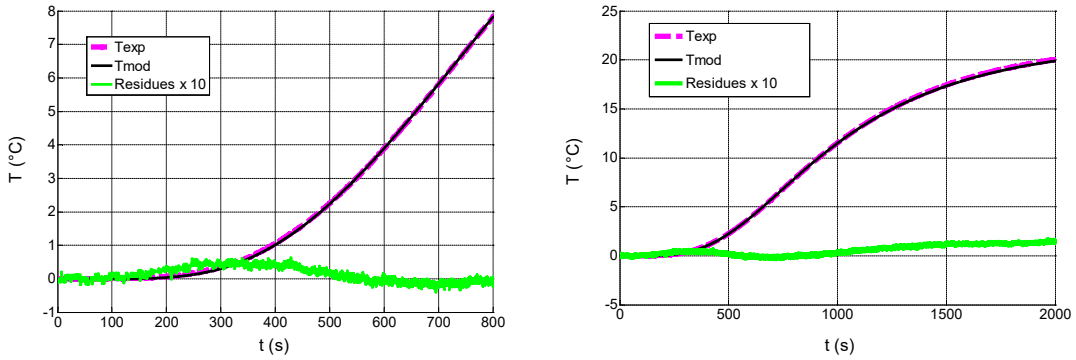

Figure 8: Examples of estimation for Silcal 1100 at 800 °C on the time intervals [0, 800s] and [0,2000s]

It should be noted that in most other transient methods at least one parameter external to the material is estimated: external transfer coefficient and absorbed energy for the flash method, for example. The adjustment of this external parameter during the estimation can sometimes compensate for a possible model bias due to the heterogeneity or semi-transparency of the material. To our knowledge, this method is the only one to estimate only one thermal parameter in the case of an opaque material, without an external adjustment parameter, which makes the shape of the residues all the more remarkable.

Table 3 presents the thermal diffusivity values estimated using:

- the thermal conductivity given by the parallel hot wire method [10] and the specific heat given by [22].
- the thermal conductivity given by the parallel hot wire method [21] and the specific heat given by [22].
- the 4L method.

The deviation remains below 11% including up to 800°C which is satisfactory given the uncertainty on the value of the thermal diffusivity calculated from the experimental data of [10], [21] and [22].

Table 3: Estimated values of the thermal diffusivity for Silcal 1100

T	4L	[10],[21]	[19],[22]	Deviation
°C	$m^2\ s^{-1}$			%
200	4.22×10^{-7}	4.23×10^{-7}	4.24×10^{-7}	-0.2
400	4.54×10^{-7}	4.93×10^{-7}	4.94×10^{-7}	-7.9
600	5.19×10^{-7}	5.79×10^{-7}	5.78×10^{-7}	-10.4%
800	6.08×10^{-7}	6.76×10^{-7}	6.77×10^{-7}	-10.5

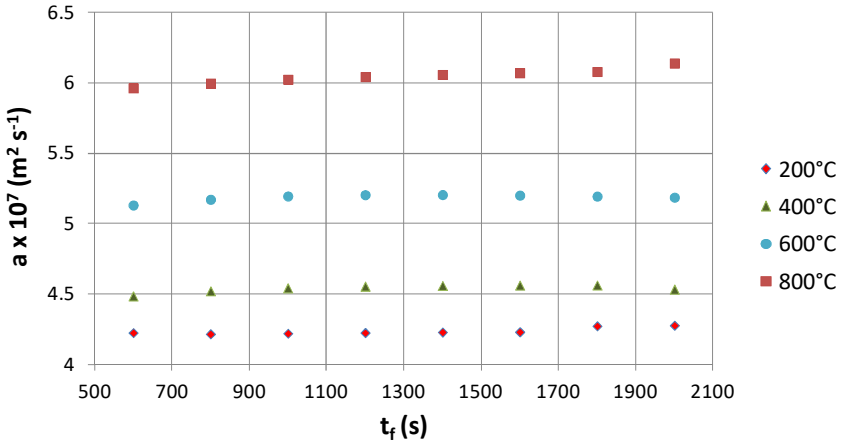

Figure 9: Estimated values of the thermal diffusivity as a function of the upper bound t_f of the estimation interval for the Silcal 1100

The robustness of the estimation of the thermal diffusivity was investigated by varying the time interval used in the inversion procedure. Figure 9 shows the estimated values of the thermal diffusivity for different upper bounds of the time interval (i.e., between 600 and 2000 s). It can be seen that the estimated value of the thermal diffusivity does not depend on the time interval chosen: whatever the temperature, the estimated value varies by less than 1% compared to the average value between 600 and 2000s.

Results for LUX 500

The results obtained for the heavier and less insulating LUX 500 are shown in Table 4 and confirm those obtained previously with Silcal 1100. The deviations from the known values for this material (cf. Table 2) remain below 4% for the three temperatures tested.

Table 4: Estimated values of the thermal diffusivity for LUX 500

	Reference (GHP + calorimetry)	Estimation (4L)	Deviation
T	a	a	
°C	m^2s^{-1}	m^2s^{-1}	%
175	3.10×10^{-7}	3.22×10^{-7}	3.3
325	3.11×10^{-7}	3.06×10^{-7}	-1.5
525	2.84×10^{-7}	2.91×10^{-7}	3.8

Results for Norfoam

An initial estimate of thermal diffusivity was made by considering the medium as opaque and using relationships (24) to (26). We deduced $\lambda = \lambda_{eq} = a\,\rho c$ by using the relation (51) to calculate the volume heat capacity ρc. As an example, Figure 10a) shows the experimental and simulated curves for Norfoam at 800°C, with residues multiplied by 10. The resulting residues are signed showing that not all physical phenomena are taken into account by the model.

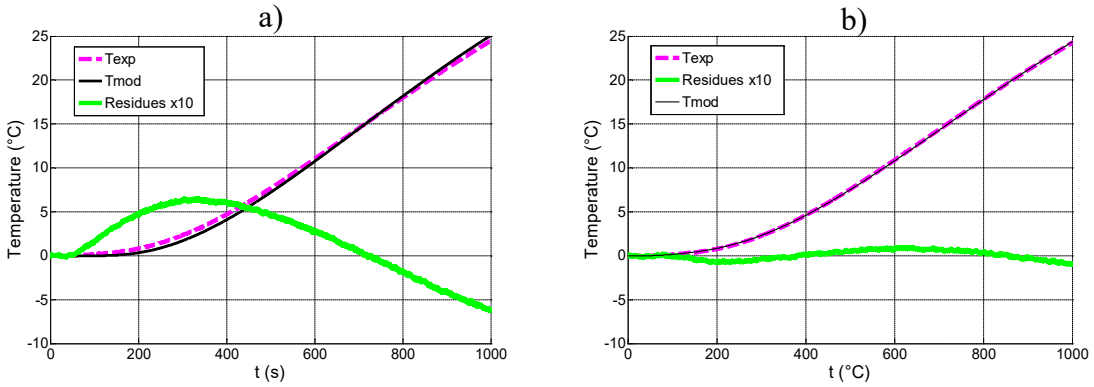

Figure 10: Experimental and estimated temperatures for Norfoam at 800°C with residues × 10: a) Purely conductive model; b) Parallel resistance model

A second estimation was therefore made by considering the presence of scattered radiation in the medium, which can be represented as a first approximation by a resistance R in parallel, using the relation (43). In this case we have estimated $a = \frac{\lambda}{\rho c}$ and $U = \frac{\lambda_r}{\lambda}$ and then used the relation (51) to calculate ρc and deduce the value of the equivalent thermal conductivity λ_{eq} by:

$$\lambda_{eq} = \lambda + \lambda_r = a\,\rho c\,(1 + U) \qquad (53)$$

Figure 10b) shows the low values of the residues, which validates the hypothesis of the purely scattering medium for Norfoam. The very slight ripples of the residues around the zero value can be explained by a low value of the coefficient of absorption, but not equal to zero.

The values of the equivalent thermal conductivity estimated by these two modes of estimation for different values of the upper bound of the time interval considered are shown in Figures 11 and 12.

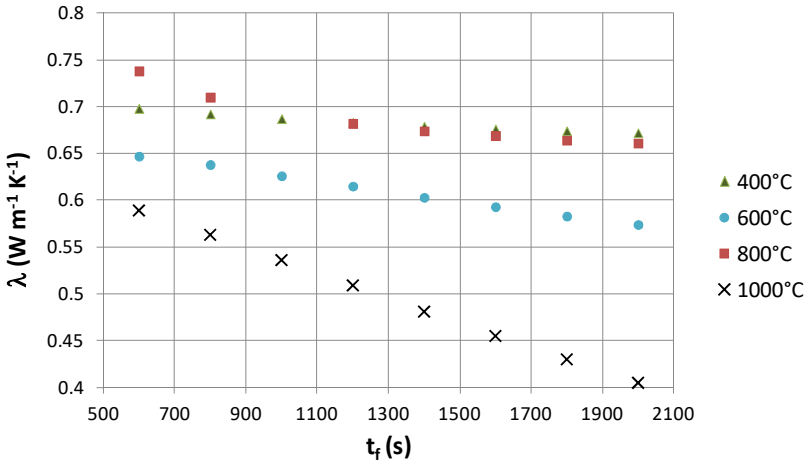

Figure 11: Estimated values of the thermal conductivity as a function of t_f with a pure conductive model

Figure 11 shows that the use of the first method does not allow the estimation of the thermal conductivity as the estimated values vary greatly with the estimation interval. On the other hand, Figure 12 shows that the estimated values of the apparent thermal conductivity vary very

slightly with the estimation interval when taking into account a resistance in parallel (relative standard deviation of 0.8%).

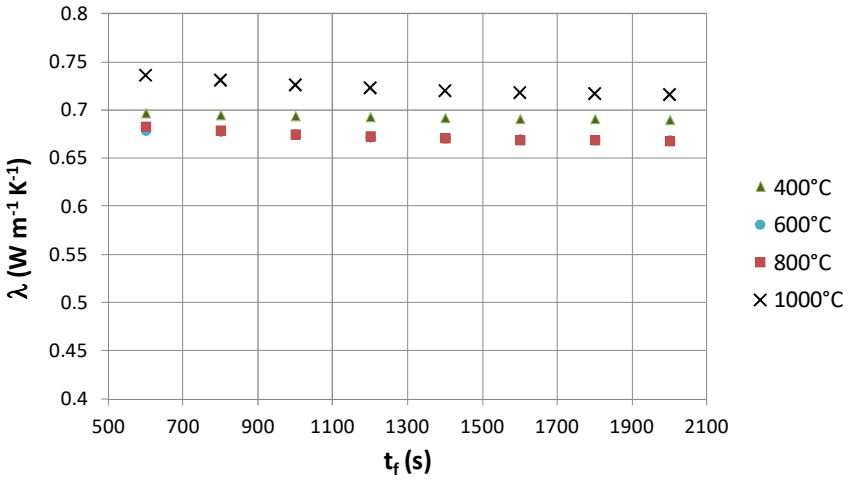

Figure 12: Estimated values of the thermal conductivity as a function of t_f with a resistance in parallel

Table 5 presents the values of the parameters estimated by the two methods over the interval [0, 1000s] as well as the values measured by the parallel hot wire method [9]. One can note that the values estimated by the 4L method with a resistance in parallel are lower than those estimated by the PHW method, the difference remaining less than 10% which can be considered satisfactory at high temperature. On the contrary, the difference between the values estimated by the 4L method with a pure conductive model or with a resistance in parallel can be very large (up to 21%). The deviation can be explained by:

- The presence of a contact resistance: it has been shown that it leads to an underestimation of the thermal diffusivity for diffusive materials.
- The fact that the thermal conductivity estimation in the PHW method was made using a purely conductive model.
- The fact that the 4L estimation was made with an approached model: pure scattering without absorption.

This discrepancy illustrates the magnitude of the error associated with the estimation of the thermal transport properties of semi-transparent materials if a purely conductive direct model is used.

Table 5: Thermal conductivity of Norfoam as a function of the temperature, estimated on 1000 s by the two models and measured values by the PHW method.

	Model used	T	°C	400	600	800	1000
4L	Pure conduction	$\lambda = \lambda_{eq}$	W m^{-1} K^{-1}	0.687	0.638	0.634	0.563
	Conduction + parallel resistance R	λ_{eq}		0.694	0.675	0.675	0.726
		λ		0.644	0.580	0.514	0.508
		λ_r		0.050	0.095	0.161	0.218
PHW	Pure conduction	λ_{eq}	W m^{-1} K^{-1}	-	-	0.75	0.80

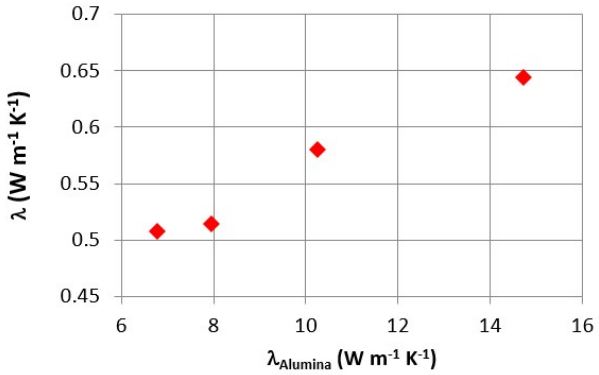

Figure 13: Phonic thermal conductivity of Norfoam as a function of Alumina thermal conductivity

Figure 13 shows that the phonic thermal conductivity λ of Norfoam varies in the same way as the thermal conductivity of Alumina and in a quasi-linear way.

For a pure scattering grey medium, the radiative conductivity can be expressed as follows [8]:

$$\lambda_r = \frac{4n^2\sigma e}{\frac{1}{\varepsilon_1}+\frac{1}{\varepsilon_2}-1+K\beta e} T^3 \quad (54)$$

where:

n optical index of the medium

σ Stefan-Boltzmann constant (W m^{-2} K^{-4})

e thickness of the medium (m)

β extinction coefficient (m^{-1}) (βe is the optical thickness of the medium)

ε_1,ε_2 emissivity of the limits of the samples

K function of βe varying between 3/4 (Deissler's approximation [26] for optically thick media) and 1 (Schuster-Schwarzschild approximation of « 2 flux » [27] for optically thin media)

Figure 14 shows the radiative conductivity estimated as a function of T^3 (T in K), which can be represented as a first approximation by a straight line passing through the origin, with a slope: $\alpha = 1.15 \times 10^{-10}$ Wm^{-1}K^{-4}. The extinction coefficient can be calculated with the formula below:

$$\beta = \frac{\frac{4n^2\sigma e}{\alpha}-\frac{1}{\varepsilon_1}-\frac{1}{\varepsilon_2}+1}{Ke} \quad (55)$$

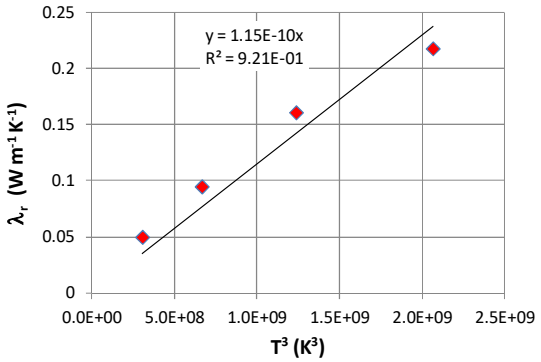

Figure 14 : Radiative conductivity as a function of T^3

Considering the values $\varepsilon_1 = \varepsilon_2 = 0.9$ and $n = 1$, we find a value $\beta = 2600$ m^{-1}, which leads to an optical thickness $\beta e = 78$. The deviation of the points from the straight line can be explained by the fact that the extinction coefficient may vary with the temperature, the value obtained is therefore an average value over the temperature range considered. The value of optical thickness is largely greater than 10 so the hypothesis of the optically thick medium is valid [10].

6. Conclusion

The novel method presented in this article is a temperature-temperature thermal characterization method for the measurement of the thermal diffusivity of insulating materials at high temperature. The method is parsimonious as it involves the estimation of only one unknown parameter, the thermal diffusivity of the material to be characterized. The method does not require the system to be at a uniform temperature at the initial time, a linear stationary temperature profile is acceptable. The ratio between the thermal contact resistance between the sample and the metallic plate and the thermal resistance of the sample must be lower than 5.6 x 10^{-3} to obtain a deviation lower than 1%.

The proposed method was validated experimentally with measurements carried out between 200 and 800°C on two different insulating materials.

An extension of the method for the characterization of purely scattering semi-transparent materials was proposed. Measurements were undertaken between 400 and 1000°C on an open-cell ceramic foam. The apparent thermal conductivity and the mean extinction coefficient of the material were estimated.

This study also highlighted the significant errors occurring if a purely conductive direct model is used for purely scattering semi-transparent materials. Further work is needed to develop a comprehensive model allowing the characterization of both absorbing-emitting and scattering semi-transparent materials.

ACKNOWLEDGMENTS

The authors would like to show their gratitude to Laurie San Miguel from Saint-Gobain Research Provence for her useful inputs and for providing Norfoam samples.

References

1. D.R. Salmon, R.P. Tye, and N. Lockmuller, A critical analysis of European standards for thermal measurements at high temperatures: I. History and technical background, Measurement Science and Technology 20 (1) (2009).
2. D.R. Salmon, R.P. Tye, and N. Lockmuller, A critical analysis of European standards for thermal measurements at high temperatures: II, Recommendations for inclusion in a new standard, Measurement Science and Technology 20 (1) (2009).
3. J. Wu , NPL In-house Designed HTGHP and LTGHP, EMRP SIB52 Thermo Stakeholder meeting, NPL, Teddington, May 16 2016, website : http://projects.npl.co.uk/thermo/docs/20160512_final_stakeholder/htghp-npl.pdf

4. LNE, Presentation of LNE's high temperature guarded hot plates, EMRP SIB52 Thermo Stakeholder meeting, NPL, Teddington, May 16 2016, website: http://projects.npl.co.uk/thermo/docs/20160512_final_stakeholder/htghp-lne.pdf
5. A.Blahut, R. Strnad, CMI high temperature guarded hot plate, EMRP SIB52 Thermo Stakeholder meeting, NPL, Teddington, May 16 2016, website: http://projects.npl.co.uk/thermo/docs/20160512_final_stakeholder/htghp-cmi.pdf
6. ISO 8302:1991. Thermal insulation – Determination of steady-state thermal resistance and related properties – Guarded hot plate apparatus (1991).
7. F. De Ponte, S. Klarsfeld, Conductivité thermique des isolants, Techniques de l'Ingénieur R 2930-17 (2002).
8. Y. Jannot and A. Degiovanni, Thermal properties measurement of materials, ISTE & Wiley Editions (2018).
9. Refractory Materials- Determination of thermal conductivity- Part 2: Hot wire method (parallel) ISO 8894-2:2007 (2007).
10. Y. Jannot, A. Degiovanni, An improved model for the parallel hot wire: application to thermal conductivity measurement of low density insulating materials at high temperature, International Journal of Thermal Sciences 142 (2019) 379-99.
11. R. Coquard , D. Baillis, D. Quenard, Experimental and theoretical study of the hot-wire method applied to low-density thermal insulators, International Journal of Heat and Mass Transfer 49 (2006) 4511-4524.
12. Hot disk- Mica sensors, website: https://www.hotdiskinstruments.com/products-services/sensors/mica-sensors/
13. G. Barth, U. Gross, R. Wulf, A new panel test facility for effective thermal conductivity measurements up to 1650°C, Proc. 17th Europ. Conf. Thermophysical Properties, Sept. 5th to 8th 2005, Bratislava, Slovakia, Paper No. 162. DOI: 10.1007/s10765-007-0272-1.
14. R. Simmat, T. Sokoll, J. Poetschke, P. Quirmbach, Thermal conductivity in the range 200 to 1600°C due to the Monotonic Heating Method, cfi/Ber. DKG 84 (9) (2007) 115-119.
15. D. Maillet, Y. Jannot, A. Degiovanni, Analysis of the estimation error in a parsimonious temperature-temperature characterization technique, International Journal of Heat and Mass Transfer 62 (2013) 230-241.
16. R. Siegel, J.R. Howell, Thermal radiation heat transfer, 2nd edition, McGraw Hill (1981).
17. S.A. Bahrani, Y. Jannot, A. Degiovanni, Extension and optimization of three-layers method for the estimation of thermal conductivity of super-insulating materials, Journal of Applied Physics 116 (14) (2014).
18. F. de Hoog, J. Knight, and A. Stokes, An Improved Method for Numerical Inversion of Laplace Transforms, SIAM Journal on Scientific and Statistical Computing 3 (3) (1982) 357–366.
19. D. Marquardt, An algorithm for least squares estimation of non-linear parameters. J. Soc. Ind. Appl. Math. 11 (1963) 431–41.
20. H. Bal, Y. Jannot, N. Quenette, A. Chenu, S. Gaye, Water content dependence of the porosity, density and thermal capacity of laterite based bricks with millet waste additive, Construction & Building Materials 31 (2012) 144-150.

21. H.P. Ebert, F. Hemberger, Intercomparison of thermal conductivity measurements on a calcium silicate insulation material, International Journal of Thermal Sciences 50 (2011) 1838-1844.
22. T. Ohmura, M. Tsuboi, M. Onodera, T. Tomimura, Specific heat measurement of high temperature thermal insulations by drop calorimeter method, International Journal of Thermophysics 24 (2) (2003) 559-575.
23. B. Hay, J. Hameury, J.-R. Filtz, F. Haloua, and R. Morice, The metrological platform of LNE for measuring thermophysical properties of materials, High Temperatures - High Pressures, 39(3) (2010).
24. Y.S. Touloukian, R.K. Kirby, R.E. Taylor, T.Y.R. Lee, Thermal expansion – Nonmetallic solids, Thermophysical Properties of Matter, Vol; 13, New York: IFI/Plenum (1984) 176-177.
25. R. Morel, Handbook of Properties of Technical & Engineering Ceramics, Part 2, Data Reviews, Section I. High-alumina ceramics, London: Her Majesty's Stationery Office (1987).
26. R. G. Deissler, Diffusion approximation for thermal radiation in gases with jump boundary condition, Journal of Heat Transfer 86 (2) (1964) 240–246.
27. S. Chandrasekhar, Radiative Transfer. Dover Publications, New York, (1960).